Proceedings of the 29th Annual International
Conference of the IEEE EMBS
Cité Internationale, Lyon, France
August 23-26, 2007.

Efficient Computer-Aided Detection of Ground-Glass Opacity Nodules in Thoracic CT Images

Xujiong Ye, Xinyu Lin, Gareth Beddoe, *Member IEEE*, Jamshid Dehmeshki, *Member IEEE*

***Abstract*—In this paper, an efficient compute-aided detection method is proposed for detecting Ground-Glass Opacity (GGO) nodules in thoracic CT images. GGOs represent a clinically important type of lung nodule which are ignored by many existing CAD systems. Anti-geometric diffusion is used as preprocessing to remove image noise. Geometric shape features (such as shape index and dot enhancement), are calculated for each voxel within the lung area to extract potential nodule concentrations. Rule based filtering is then applied to remove False Positive regions. The proposed method has been validated on a clinical dataset of 50 thoracic CT scans that contains 52 GGO nodules. A total of 48 nodules were correctly detected and resulted in an average detection rate of 92.3%, with the number of false positives at approximately 12.7/scan (0.07/slice). The high detection performance of the method suggested promising potential for clinical applications.**

I. Introduction

THERE has been growing interests in developing Computer-Aided Detection (CAD) technology with Computer Tomography (CT) for lung cancer, which is the main cause of cancer deaths. Lung nodules can be classified into two categories: solid nodules characterized by their high contrast and Ground-Glass Opacity (GGO) nodules with faint contrast and fuzzy margins [1]-[3]. Studies on lung nodule CAD are reported frequently in the literature. However, most of the work has been focused on solid nodule detection only. GGO nodule detection remains one of the major difficulties in CAD development. This paper describes a new CT lung CAD method which aims to detect GGO nodules.

Lung CAD techniques in the literature can be divided into two groups [4]: intensity based and model based methods. Intensity based detection methods are usually based on the assumption that lung nodules have relatively higher intensity than those of lung parenchyma, employing techniques such as multiple thresholding [5], local adaptive thresholding [6] etc, to identify nodules in lung area. The model based methods employ techniques (such as template-matching [7], object-based deformation [8] etc) to separate spherical shaped nodules from elongated structures.

The purpose of this paper is to propose a new and effective approach to lung CAD which uses 3D local geometry and statistical intensity features for GGO nodule extraction. The most closely related research to our own is that by Yoshida [9], in which shape index is calculated on each 3D voxel within the segmented lungs. However, there are several major differences. Firstly, in our paper, anti-geometric diffusion, which diffuses image across the image edges, is used as a preprocessing step to remove the noise and enhance the image. The smoothness of the edge generated by anti-geometric diffusion is better suited to the accurate calculation of voxel based geometric features. Secondly, apart from using the shape index feature to generate initial potential nodule candidates, the Dot map is calculated, based on the eigenvalues of Hessian matrix for each voxel, and used to simultaneously enhance the objects of a specific shape (such as dot-like nodule object), and suppress object of other shapes (such as line-like vessel object). Thirdly, an adaptive thresholding method based on the intensity statistics of the low sphericity concentration is employed to efficiently segment potential nodule objects. Rule-based filtering is finally applied as a main false positive (FP) reduction step to quickly remove easily dismissible FP objects.

II. Methodology

Fig.1 provides a summary of the proposed automatic lung GGO nodule detection scheme.

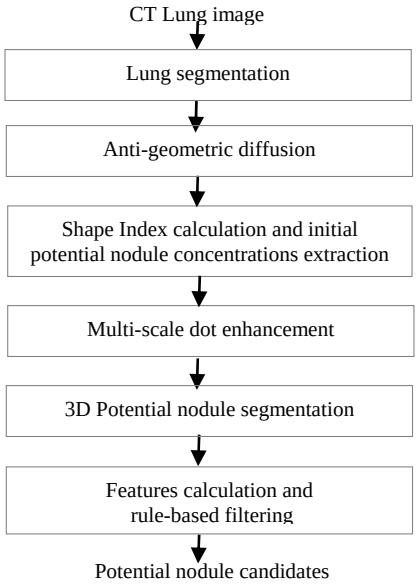

Fig.1 Flow diagram of proposed GGO nodule detection system

A. Lung Segmentation

Lung segmentation consists of two stages: Initial lung

X. Ye, X. Lin, G. Beddoe are employed by Medicsight PLC, 66 Hammersmith Road, London W14 8UD, UK.(xujiong.ye@medicsight.com).
J. Dehmeshki was employed by Medicsight PLC, now is with Kingston University, London, KT1 2QJ, UK.

contour generation and lung contour refinement. In the first stage, an adaptive fuzzy thresholding value, which is calculated based on the cumulative histogram and first moment of image Hunsfield Unit (HU), is used to segment the lung parenchyma [10]; In the second stage, the initial lung contour is further refined based on the detection of the concave regions from the critical points. Fig. 2 shows the results of the segmented lung mask on one real CT image with a nodule attached to the lung wall.

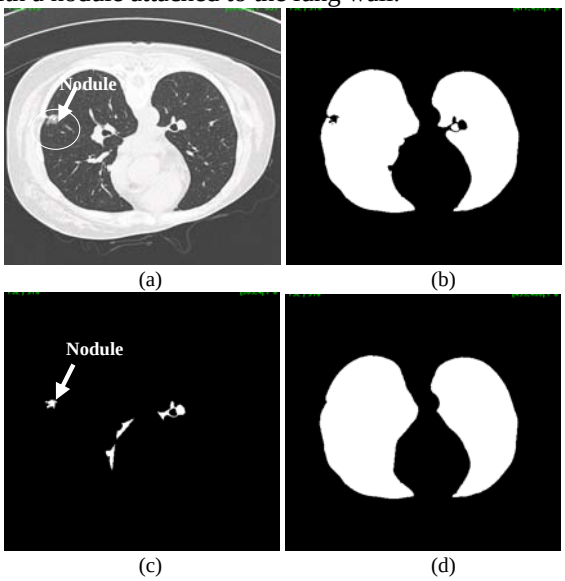

Fig. 2 Lung segmentation based on fuzzy thresholding method. (a) Original CT lung image; (b) Initial lung mask extraction; (c) Segmented concave regions (an attached nodule and other attached tissues) based on critical points on the initial contour; (d) Final segmented lung mask.

B. Anti-Geometric Diffusion

An anti-geometric diffusion model proposed by Siddharth, *et al* [11] is used as a preprocessing step to remove noise and enhance the image. Given iso-intensity contours (level curves) of an image $I(x,y,z)$, with η and ξ denoting gradient and tangent directions respectively, the anti-geometric diffusion can be defined as:

$$\frac{\partial I}{\partial t} = \frac{I_x^2 I_{xx} + 2I_x I_y I_{xy} + I_y^2 I_{yy}}{I_x^2 + I_y^2} \tag{1}$$

While the traditional geometric diffusion model diffuses the image along the image edges, the anti-geometric diffusion model diffuses across image edges. The advantages of diffusing across image edge include better localization, less sensitivity to noise, and better connectivity. The smoothness of the edge is very important for the accurate voxel based geometry feature calculations which will be discussed in the next section.

C. Shape Index: A 3D Geometric Feature for Potential Nodule Detection

A 3D geometric feature, volumetric shape index [12], is calculated for each voxel to extract the potential nodule candidates. This is based on the fact that an isolated nodule or a nodule attached to a blood vessel is generally either depicted as a sphere or has some spherical elements, while a blood vessel is usually oblong.

The volumetric shape index [12] at voxel $p(x,y,z)$ can be defined as:

$$SI(p) = \frac{1}{2} - \frac{1}{\pi}\arctan\frac{k_1(p)+k_2(p)}{k_1(p)-k_2(p)} \tag{2}$$

where $k_1(p)$ and $k_2(p)$ are the principal curvatures at voxel *p*, which are calculated based on Gaussian and mean curvatures [9] [12].

Shape index is a very useful feature. Theoretically, it represents the local shape feature at each voxel while being independent of the image intensity. This feature is advantageous here because it can be used for detecting low contrast GGO nodules. To illustrate the characteristics of the shape index, Fig. 3(a) and (b) show an original lung image and its corresponding shape index map, Fig. 3(c) and (d) are highlighted shape index values on one nodule and one blood vessel, respectively. It is noted that the average of the shape index values for the nodule is higher than that of the blood vessel. A hysteresis thresholding [9] is then applied to extract potential nodule candidates as shown in Fig. 4(b).

Fig. 4 demonstrates that the shape index feature is capable of detecting the sphere-like GGO nodule elements. However, some non-nodule objects with high sphericity elements (e.g. joining of vessels) are also detected as shown in Fig. 4(b). The following Dot Enhancement filtering is proposed to remove those non-nodule objects.

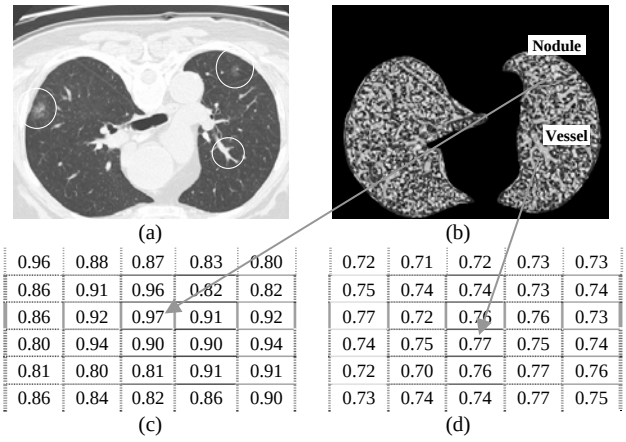

Fig. 3 An example of shape index map with GGO nodules (a) Original lung image; (b) Shape index map; (c) Shape index values for sphere-like nodule; (d) Shape index values for cylinder-like blood vessel

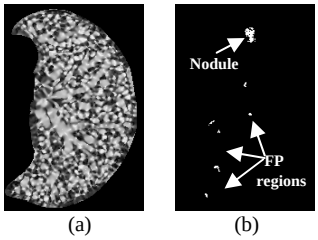

Fig. 4 An example of potential nodule regions extraction. (a) Shape index map from right lung in Fig.3(b); (b) Detected potential nodule candidates.

D. Multi-Scale Dot Enhancement Filtering

The Dot enhancement (DE) algorithm is used to simultaneously enhance objects of a specific shape (such as dot-like objects), and suppress objects of other shapes (such as line-like objects). The dot value is defined as [13]:

$$D_{dot}(\lambda_1,\lambda_2,\lambda_3)=\begin{cases}|\lambda_3|^2 \big/ |\lambda_1| & \text{if } \lambda_1<0,\lambda_2<0,\lambda_3<0\\ 0 & \text{Otherwise}\end{cases} \quad (3)$$

where λ_1, λ_2 and λ_3 are three eigenvalues from a 3×3 Hessian matrix which is calculated based on the second derivatives.

In this paper, a dot map is calculated on each potential nodule region obtained from the shape index map, in which three Gaussian scales with a range of $[0.5,2.5]$ are used. For each potential nodule candidate $\Re_{sl}$, we calculate:

$$\sum_{i\in\Re_{sl}} S(D^i_{dot}-\vartheta_d)>\vartheta_{count} \quad (4)$$

where, D^i_{dot} is the dot value at *i*th voxel in $\Re_{sl}$ region calculated based on (3), ϑ_d is a pre-defined threshold for the dot value in the DE map, ϑ_{count} is a pre-defined threshold for the number of voxels whose dot values are larger than ϑ_d, and $S(x)=\begin{cases}1, & \text{if } x\ge0\\ 0, & \text{otherwise}\end{cases}$.

The region $\Re_{sl}$ is kept as a potential nodule candidate if it satisfies the condition set in (4), otherwise the region is considered to be an FP region.

E. Potential Nodule Segmentation Based on an Adaptive Thresholding Method

An adaptive thresholding method is used on the extracted sub-image from the potential nodule concentration ($\Re_{sl}$) to efficiently segment low contrast GGO nodules.

Two intensity thresholds are calculated as follows:

$$f_{Thldlow}=f_{Mean}-|f_{\min}-f_{Mean}|\times0.1$$
$$f_{Thldhigh}=f_{Max}-|f_{\min}-f_{Max}|\times0.1 \quad (5)$$

where, f_{Mean} and f_{Max} are the mean and maximum intensities in the region $\Re_{sl}$, respectively. $f_{\min}$ is the minimum intensity in the sub-image.

Fig. 5 shows the segmented potential nodule based on the adaptive thresholding method. Fig. 5(b) is one cross-section of the nodule concentration mask $\Re_{sl}$ which was calculated from the shape index map. The mean and minimum intensity values used in (5) are calculated based on this mask. A 3D labeling technique is applied on the segmented image and the region which has the largest overlap with the concentration mask is used as the final segmented nodule object as shown in Fig. 5(c). The adaptive thresholding is a fast segmentation method. The thresholds for the nodule segmentation are estimated based on the intensity statistics (such as mean and maximum intensities) of the region concentration**.** In the case of low contrast GGO nodules which usually have smaller intensity variance within the nodule objects, the intensity statistics from $\Re_{sl}$ are similar to that of the segmented nodule. This is the main reason that the fast algorithm is suitable for low contrast GGO nodule segmentation.

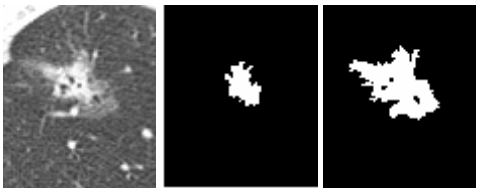

(a) (b) (c)

Fig. 5 Potential nodule segmentation based on adaptive thresholding; (a) One cross-section of 3D GGO nodule image; (b) Potential nodule concentration $\Re_{sl}$ from shape index map; (c) Segmented nodule region

F. Rule-based Filtering to Remove False Positive Regions

Geometric shape features are calculated on each segmented potential nodule object $\Re_{seg}$. Rule-based filtering is then applied to further remove FP regions.

1) 3D Maximum distance to the boundary

For each potential nodule object, a 3D distance map is calculated based on the distance transform technique [14]. The maximum distance value to the boundary within the object can be used to remove very thin objects. For example, the *i*th region $\Re_{seg}$ is kept as a potential nodule candidate if $fDisMax_i>\vartheta_{dis}$, where $fDisMax_i$ is the maximum distance value for *i*th object and ϑ_{dis} is a pre-defined threshold for object thinness.

2) 3D Object filtering based on motion tracking

Assuming 3D object contains more than one 2D blob (a blob is a cross-section defined in x-y plane) along the scanning (z) direction, an object is defined as a blob-moving object if its 2D blobs on different continuous slices are moving along x-y plane. The blob-moving object characteristic indicates a potential blood vessel. Fig. 6 shows an example of a blob-moving object. For each 2D blob, a kernel is calculated based on the distance transform technique. By measuring the degree of overlapping consecutive 2D kernel regions along the scanning direction, the blob-moving objects can be detected and removed from nodule candidates.

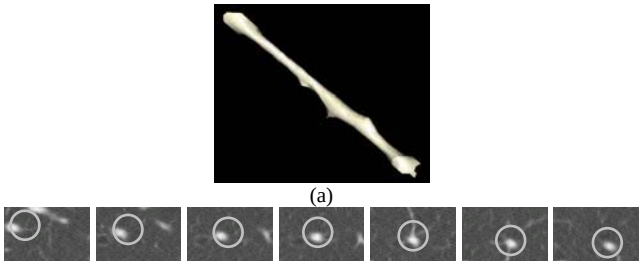

(a)

(b)

Fig. 6 An example of a blob-moving object; (a) 3D view of the object (b) 2D view of each blob on different continuous slices (along scan direction).

3) Other local features

Apart from the two main features mentioned above, other local features of the segmented object, such as volume size, sphericity, compactness, maximum and minimum HU are also calculated for the rule-based filtering.

III. Experimental results

A database of 50 thoracic CT scans was used to evaluate the effectiveness of the proposed method. Each scan was read individually by three experienced thoracic radiologists to produce a gold standard of 52 GGO nodules (part-solid and non-solid), with diameters ranging from 4mm to 20mm. Slice thickness varied from 1.0mm to 2.0mm and the total slice number for each scan varied from 124 to 316 with an average of 172 per-scan. The X-ray tube current ranged from 60mA to 325mA. Table 1 summarizes the performance of the proposed method. 48 of 52 GGO nodules were detected with an average detection rate of about 92.3% and false positive rates of approximately 12.7/scan (0.07/slice).

Fig. 7 shows examples of different types of detected GGO nodules. As discussed in section II, a high spherical concentration can be obtained by thresholding the shape index map. Therefore, different shape index thresholds produce different nodule detection performances (detection sensitivities and specificities). Fig. 8 shows the method's performance for 11 different high shape index thresholds, ranging from 0.89 to 0.99. It is noted that a shape index thresholding value of 0.91 provides an optimal overall performance with a higher detection rate (about 92.3%) and a relatively small FP rate (about 0.07/slice).

Table 1 GGO Nodule detection performance (on a database of 50 scans with 52 GGO nodules)

Methods	Nodule detected	Detection rate	FP Per-scan
Proposed method	48	92.3%	12.7/scan (0.07/slice)

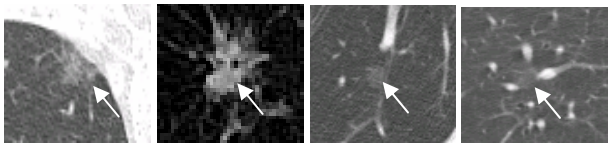

Fig. 7 Low contrast GGO nodules detected by the proposed method

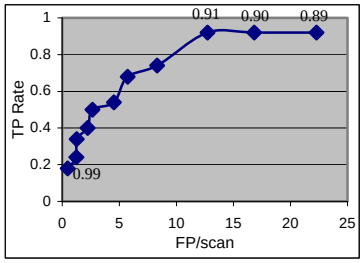

Fig. 8 Performance evaluation for GGO nodules with 11 different high shape index thresholding values ranging from 0.89 to 0.99.

IV. Conclusions

In this paper, a shape-based method is proposed for the detection of GGO nodules. Anti-geometric diffusion is used as a pre-processing step for image enhancement which provides a solid foundation for the accurate calculation of voxel based geometric features. The shape features characterize the local geometric information while being independent of image intensity. This is the main reason that the proposed algorithm is able to detect not only non-spherical GGO nodules containing spherical elements, but also the very low contrast GGO nodules. An adaptive thresholding method is employed to efficiently segment the potential nodule objects and rule-based filtering is finally used to further remove false positive regions.

The high performance of the proposed method with respect to sensitivity of 92.3% and FP at 0.07/slice provides a good basis for a lung GGO CAD system and suggests promising potential for clinical application.

References

[1] H. Kim, M. Maekado, J.K.Tan, S.Ishikawa and M.Tsukud, "Automatic extraction of ground-glass opacity shadows on CT Images of the thorax by correlation between successive slices", *Proc. Intl., on Tools with Artificial Intelligence (ICTAI)*, 2005.

[2] H.A.Bastawrous, T.Fukumoto, N.Nitta and M.Tsudagawa, "Detection of Ground Glass Opacities in Lung CT Images using Gabor Filters and Neural Networks", *Proc. Intl., on Instrumentation and Measurement Technology (IMTC)*, pp.251-256, 2005.

[3] S.Matsumoto, Y.Ohno, H.Yamagata, H.Asahina, K.Sugimura: A new scheme for computer-aided detection of CT lung nodules designed in consideration of ground-glass opacity. *Int J CARS* (2006) 1:345-367.

[4] I.Sluimer, A.Schilham, M.Prokop B.V.Ginneken: Computer analysis of computed tomography scans of the lung: A survey. *IEEE Trans. Medical Imaging*, vol.25 (2006) 385-405.

[5] S.G. Armato, M. L. Giger and H. MacMahon, ''Automated detection of lung nodules in CT scans: Preliminary results'', *Med. Phys*. vol.28, pp.1552–1561, 2001.

[6] L. Fan, C. Novak and J. Qian, et al., "Automatic detection of lung nodules from multi-slice low-dose CT images", *Proc. SPIE*, vol.4322, pp.1828-1835, 2001.

[7] Y. Lee, T. Hara and H. Fujita, S.Itoh, and T.Ishigaki, "Automated detection of pulmonary nodules in helical CT images based on an improved template-matching technique", *IEEE Trans. on Medical Imaging*, vol.20, no.7, pp.595-604, 2001.

[8] S. Lou, C. Chang, K. Lin, T. Chen. Object-based deformation technique for 3-D CT lung nodule detection. *Proc. SPIE*, vol.3661, pp.1544-1552, 1999.

[9] H.Yoshida and J. Nappi, "Three-dimensional computer-aided diagnosis scheme for detection of colonic polyps", *IEEE Trans. Medical Imaging*, vol.20, no.12, pp.1261-1273, 2001.

[10] Hamid R.Tizhoosh: Fuzzy Image Processing. Springer-Verlag, 1997.

[11] S. Manay, A.Yezzi, "Anti-geometric diffusion for adaptive thresholding and fast segmentation", *IEEE Trans. Image Processing*, vol.12, no.11, pp.1310-1322, 1003.

[12] O. Monga, S. Benayoun. "Using partial derivatives of 3D images to extract typical surface features", *Computer Vision and Image Understanding*, vol.61, pp.171-189, 1995.

[13] Q. Li, S. Sone and K. Doi, "Selective enhancement filters for nodules, vessels, and airway walls in two- and three-dimensional CT scans", *Medical Physics*, vol.30, no.8, pp.2040-2051, 2003.

[14] R.C, Gonzalez and R.E: Woods, Digital Image Processing. Addison Wesley, 2nd edition, 2002.